A THREE DIMENSIONAL STAGGERED GRID PRIMITIVE EQUATION MODEL FOR APPLICATION TO MESOSCALE ATMOSPHERIC MOTIONS

Robert Bozich

NAVAL POSTGRADUATE SCHOOL
Monterey, California

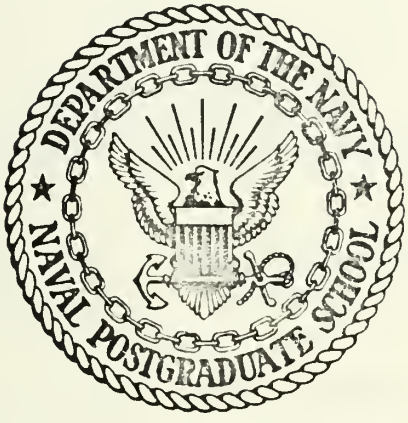

THESIS

A Three Dimensional Staggered Grid Primitive Equation Model for Application to Mesoscale Atmospheric Motions

by

Robert Bozich

Thesis Advisor: Ronnie L. Alberty

March 1972

A Three Dimensional Staggered Grid Primitive Equation Model for Application to Mesoscale Atmospheric Motions

by

Robert Bozich
Lieutenant, United States Navy
B.S., Meteorology, Pennsylvania State University, 1964

Submitted in partial fulfillment of the
requirements for the degree of

MASTER OF SCIENCE IN METEOROLOGY

from the

NAVAL POSTGRADUATE SCHOOL
March 1972

ABSTRACT

A three dimensional staggered grid model, based on the Boussinesq equations, is developed, and applied to mesoscale waves. The model is tested with a three dimensional stable gravity wave and forecasts for 40 time steps are compared with the analytical solutions and also with a full grid model. Comparisons show very good agreement with both forecasts for the stated time. Failure of the relaxation scheme to meet the convergence criterion after 47 time steps is discussed.

TABLE OF CONTENTS

LIST OF FIGURES

LIST OF SYMBOLS AND ABBREVIATIONS

c	Phase speed of disturbance (m sec^{-1}).
c_p	Specific heat of air at constant pressure (joule $gm^{-1}{}^{\circ}K^{-1}$).
f	Coriolis parameter (sec^{-1}).
f_o	Constant Coriolis parameter ($.8365 \times 10^{-4}$ sec^{-1}).
F	Forcing function for the relaxation equation.
g	Acceleration due to gravity (m sec^{-2}).
i	Grid index in x direction
IM	Number of grid points in the x direction.
j	Grid index in y direction.
JM	Number of grid points in the y direction.
k	Grid index in z direction.
KM	Number of grid points in the z direction.
λ	Wave number in the x direction = $2\pi/L_x$.
L_x	Wave length in the x direction.
L_y	Wave length in the y direction.
L_z	Wave length in the z direction.
m	Wave number in the z direction = π/L_z.
P	Pressure (mb).
P_o	1000 (mb).
R	Gas constant for air (joule $gm^{-1}{}^{\circ}K^{-1}$).
S	Used to denote any arbitrary scalar quantity
t	Time (sec).
T	Temperature (°K).
u	x component of horizontal velocity (m sec^{-1}).
v	y component of horizontal velocity (m sec^{-1}).

$\overline{V}_3$ Three dimensional wind vector.

w Vertical component of velocity (m sec^{-1}).

W Scale value of vertical motion.

Δx Mesh length in the x direction.

Δy Mesh length in the y direction.

Δz Mesh length in the z direction.

ζ Vertical component of relative vorticity (sec^{-1}).

θ Deviation from adiabatic potential temperature (°K).

θ_o 300 (°K).

$\overline{\theta}$ Stratification potential temperature (°K).

Θ Potential temperature (°K).

κ R/c_p.

μ Wave number in the y direction = π/L.

ν Kinematic viscosity coefficient ($m^2 sec^{-1}$).

β Pressure parameter.

β_o Hydrostatic part of the pressure parameter.

β' Non-hydrostatic part of the pressure parameter.

ρ Density of air (kgm m^{-3}).

∇ Del operator = $\overline{i}\frac{\partial}{\partial x} + \overline{j}\frac{\partial}{\partial y} + \overline{k}\frac{\partial}{\partial z}$.

∇_3^2 Laplacian operator = $\frac{\partial^2}{\partial x^2} + \frac{\partial^2}{\partial y^2} + \frac{\partial^2}{\partial z^2}$.

$\dot{\nabla}_2$ Finite difference form of the del operator.

ACKNOWLEDGMENT

The author wishes to express his gratitude to Dr. R. L. Alberty, whose suggestion it was to undertake this project, and whose unfailing optimism, infinite patience and thorough understanding of the subject of atmospheric convection contributed greatly to the completion of this project. Thanks also go to Drs. R.T. Williams and R.L. Elsberry for discussions of dynamics and finite differencing schemes used in the program and also to Dr. Williams for his careful review of the original manuscript. Computer time for the numerical calculations was provided by the W.R. Church Computer Center at the Naval Postgraduate School.

I. INTRODUCTION

In the past few years many attempts have been made to understand the complex dynamic interactions between the thunderstorm and its environment. Newton and Newton (1959) proposed a dynamical thunderstorm model which proposed that strong vertical motions within the thunderstorm cell create an effective barrier to the flow of the environmental air.

Ogura (1963) first discussed the probability of using the primitive equations for forecasting small scale dynamical features. Interaction between the convective elements and the environmental wind field can be investigated numerically by the use of these equations. Deardorff (1970) made a numerical study of turbulent flow using a three-dimensional primitive equation model. A similar forecasting procedure is used in this model. The importance of gravity waves in small scale convective activity is discussed by Matsumoto and Ninomiya (1969). Orszag (1969) presented a model for the simulation of turbulence which employs a fast Fourier Transform instead of the Liebmann Relaxation Technique. Further refinement of this model may be accomplished by the use of such a method.

Norton (1970) discussed the development of a three dimensional model for application to mesoscale motions based on the Boussinesq equations. The model presented here is a further development of the same model with a staggered grid system applied to minimize computer storage requirements. The total grid size is 14 by 14 in the horizontal with 10 levels in the vertical, while the computational grid size is 11 by 10 by 6. The grid

interval in all directions is 1 kilometer. The Coriolis parameter, treated as a constant, is determined at a mean latitude of 35° North.

Numerical computations are made using the IBM OS/360 Computer of the W. R. Church Computer Center. To conform to computational stability a time step of 30 seconds was chosen.

II. MODEL DEVELOPMENT EQUATIONS

A. FORECAST EQUATIONS

The pressure term in the complete equation of motion can be written as:

$$\frac{1}{\rho} \nabla_3 p = \frac{RT}{p} \nabla_3 \left[\frac{p_o}{C_p^{1/\kappa}} \beta^{1/\kappa} \right]$$

or

$$\frac{1}{\rho} \nabla_3 p = \Theta \nabla_3 \beta$$

where

$$\beta = C_p \left[\frac{p}{p_o} \right]^{\kappa}$$

and

$$\Theta = T \left[\frac{p_o}{p} \right]^{\kappa}$$

Using these results in the component form of the equation of motion yields:

$$\frac{du}{dt} = - \Theta \frac{\partial \beta}{\partial x} + fv + \nu \nabla_3^2 u \quad , \tag{1}$$

$$\frac{dv}{dt} = - \Theta \frac{\partial \beta}{\partial y} - fu + \nu \nabla_3^2 v \quad , \tag{2}$$

$$\frac{dw}{dt} = - \Theta \frac{\partial \beta}{\partial y} - g + \nu \nabla_3^2 w \quad . \tag{3}$$

The perturbation expressions can be formed by:

$$\beta = \beta_o(z) + \beta'(x,y,z,t)$$

$$\theta = \theta_o + \theta(x,y,z,t)$$

where

$$|\beta'| << \beta \qquad \text{and} \qquad |\theta| << \theta_o$$

and the latter inequality corresponds to the Boussinesq approximation.

After substitution into equations (1), (2), and (3), the equations of motion can be written:

$$\frac{du}{dt} = -\theta_o \frac{\partial \beta'}{\partial x} + fv + \nu \nabla_3^2 u, \tag{4}$$

$$\frac{dv}{dt} = -\theta_o \frac{\partial \beta'}{\partial y} - fu + \nu \nabla_3^2 v, \tag{5}$$

and

$$\frac{dw}{dt} = -\theta_o \frac{\partial \beta_o}{\partial z} - \theta_o \frac{\partial \beta'}{\partial z} - \theta \frac{\partial \beta_o}{\partial z} - g + \nu \nabla_3^2 w .$$

with the relatively small products:

$$\theta \frac{\partial \beta'}{\partial x} , \ \theta \frac{\partial \beta'}{\partial y} , \text{ and } \theta \frac{\partial \beta'}{\partial z}$$

being neglected. The hydrostatic equation relates β_o and θ_o by:

$$\frac{\partial \beta_o}{\partial z} = - \frac{g}{\theta_o}$$

and the vertical component can now be written:

$$\frac{dw}{dt} = - \theta_o \frac{\partial \beta'}{\partial z} + \frac{g\theta}{\theta_o} + \nu \nabla_3^2 w \tag{6}$$

By defining $\phi = \theta_o \beta'$ and substituting into (4), (5), and (6) and expanding the total derivatives, the system of equations becomes:

$$\frac{\partial u}{\partial t} = -L(u) - \frac{\partial \phi}{\partial x} + fv + \nu \nabla_3^2 u, \tag{7}$$

$$\frac{\partial v}{\partial t} = -L(v) - \frac{\partial \phi}{\partial y} - fu + \nu \nabla_3^2 v, \tag{8}$$

$$\frac{\partial w}{\partial t} = -L(w) - \frac{\partial \phi}{\partial z} + \frac{g\theta}{\theta_o} + \nu \nabla_3^2 w, \tag{9}$$

$$\frac{\partial \theta}{\partial t} = -L(\theta) \quad , \tag{10}$$

$$\nabla_3 \cdot \overline{V} = 0 \quad . \tag{11}$$

where $L(S) = - \nabla_3 \cdot (\overline{V}_3 S), \quad S = u,v,w,\theta$.

Incompressible flow is assumed, to eliminate sound waves. This system has become known as the anelastic equations and are quite accurate for shallow convection. (Ogura and Phillips, 1962)

B. DETERMINATION OF THE PRESSURE TERMS

Equations (7), (8), and (9) may be combined in vector form and written:

$$\frac{\partial \overline{V}_3}{\partial t} = -(\overline{V}_3 \cdot \nabla)\overline{V}_3 - \nabla_3\phi - f(\overline{k} \times \overline{V}_3) + \frac{g\theta}{\theta_o}\overline{k} + \nu \nabla_3^2 \overline{V}_3 \qquad (12)$$

By taking the three dimensional divergence and assuming the time rate of change to be zero, (12) becomes:

$$\begin{aligned} \frac{\partial}{\partial t}(\nabla_3 \cdot \overline{V}_3) &= 0 \\ &= -\nabla_3 [(\overline{V}_3 \cdot \nabla_3)\overline{V}_3] - \nabla_3^2\phi \\ &\quad -\nabla_3 \cdot [f(\overline{k} \times \overline{V}_3)] + \frac{g}{\theta_o} \frac{\partial \theta}{\partial z} + \nabla_3 \cdot \nu \nabla_3^2 \overline{V} \end{aligned} \qquad (13)$$

For the horizontal extent used in this model, the Coriolis parameter may be treated as a constant and then (13) becomes:

$$\begin{aligned} \nabla_3^2\phi &= -\nabla_3 \cdot [(\overline{V}_3 \cdot \nabla_3)\overline{V}_3] - f_o \nabla_3 \cdot (\overline{k} \times \overline{V}_3) + \frac{g}{\theta_o} \frac{\partial \theta}{\partial z} \\ &= -\nabla_3 \cdot [(\overline{V}_3 \cdot \nabla_3)\overline{V}_3] + f_o \zeta + \frac{g}{\theta_o} \frac{\partial \theta}{\partial z} + \nabla_3 \cdot \nu \nabla_3^2 \overline{V} \end{aligned} \qquad (14)$$

Note that when the terms on the RHS are solved by ordinary differencing techniques, the value of ϕ on the LHS can be solved by using the Extrapolated Liebmann Relaxation Scheme.

III. FINITE DIFFERENCING

Numerical integration of equations (7) through (10) is carried out using finite difference methods in x,y,z, and t. Extrapolated Liebmann Relaxation is used to solve for the pressure term in equation (14). For the complete development of the relaxation scheme, see Appendix A. The technique applied to generate the forcing function used in (14) is shown in complete form in Appendix B.

To maintain consistency in finite differencing throughout the forecast procedure, the differencing scheme used in equation (14) must be equivalent to the type used on equations (7), (8), and (9). The flux form differencing method devised by Arakawa (1966) was utilized in the form:

$$
\begin{aligned}
L(S)_{i,j,k} = & \Big[(u_{i+1,j,k} + u_{i,j,k})\,(S_{i+1,j,k} + S_{i,j,k}) \\
& -(u_{i-1,j,k} + u_{i,j,k})\,(S_{i-1,j,k} + S_{i,j,k})\Big] / 4\Delta x \\
& +\Big[(v_{i,j+1,k} + v_{i,j,k})\,(S_{i,j+1,k} + S_{i,j,k}) \\
& -(v_{i,j-1,k} + v_{i,j,k})\,(S_{i,j-1,k} + S_{i,j,k})\Big] / 4\Delta y \\
& +\Big[(w_{i,j,k+1} + w_{i,j,k})\,(S_{i,j,k+1} + S_{i,j,k}) \\
& -(w_{i,j,k-1} + w_{i,j,k})\,(S_{i,j,k-1} + S_{i,j,k})\Big] / 4\Delta z
\end{aligned}
$$

This method is used for the u,v,w and Θ fields, but for the linear space derivatives for ϕ, an averaging technique must be employed due to the staggered grid system. The centered form of the space derivative takes on the form:

$$\left(\frac{\partial S}{\partial x}\right)_{i',j',k'} = \Big[(S_{i,j,k} + S_{i,j,k-1} + S_{i,j-1,k} + S_{i,j-1,k-1}) / 4.$$

$$-(S_{i-1,j,k} + S_{i-1,j,k-1} + S_{i-1,j-1,k} + S_{i-1,j-1,k-1})/4.\Big]/\Delta x$$

with similar forms for the y and z derivatives. The primed subscripts refer to the grid points one-half grid distance above or below the diagonals connecting surrounding velocity points in a horizontal plane. Centered time differencing ("leapfrog") is used for all forecasts with the exception of the first time step where a single forward time step is used.

IV. BOUNDARY CONDITIONS

The boundary conditions are selected to enforce mass and energy conservation within the confines of the computational grid. Figure 1 illustrates the horizontal grid domain and boundary placement. Cyclic continuity of parameters is imposed by forcing periodicity in the east-west direction according to the relations

$$S_{1,J,K} = S_{IM-2,J,K}$$

$$S_{2,J,K} = S_{IM-1,J,K}$$

$$S_{IM,J,K} = S_{3,J,K}$$

where S = u,v,w, θ. Since values of S are required at three consecutive points in solving for the pressure and divergence terms, values outside the domain can be obtained through the cyclic conditions. The east-west boundary conditions on ϕ are also cyclic and are specified by:

$$\phi_{1,J,K} = \phi_{IM-2,J,K}$$

$$\phi_{IM-1,J,K} = \phi_{2,J,K} \quad .$$

The south boundary is located halfway between velocity grid points J = 2 and J = 3, while the north boundary is between the points J = JM - 2 and J = JM - 1. To prevent the flow of mass and energy through these boundaries, the v-component is set by the following conditions:

$$V_{I,1,K} = -V_{I,4,K}$$

$$V_{I,2,K} = -V_{I,3,K}$$

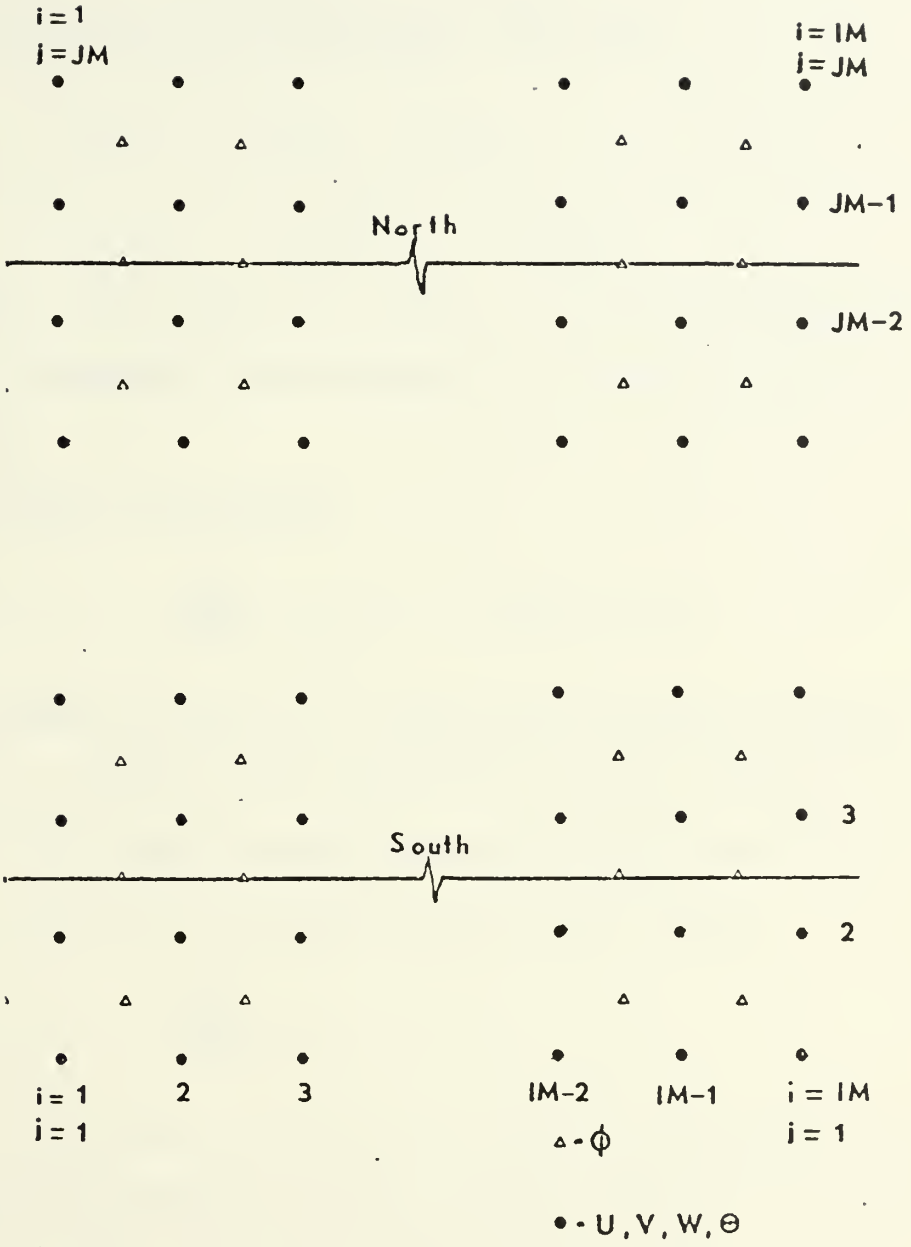

Figure 1. Illustration of the grid system in the horizontal direction.

$$V_{I,JM,K} = -V_{I,JM-3,K}$$

$$V_{I,JM-1,K} = -V_{I,JM-2,K} \quad .$$

The values of u,w, and θ are extrapolated outward by:

$$S_{I,1,K} = S_{I,2,K} = S_{I,3,K}$$

$$S_{I,JM,K} = S_{I,JM-1,K} = S_{I,JM-2,K}$$

where S = u,w,θ. This implies that there is no advection through this boundary and furthermore no heat exchange as discussed by Ukaji and Matsuno (1970).

The geostrophic relationship:

$$\left(\frac{\partial \phi}{\partial y}\right)_{i',j',k'} = - f_o \, u^*_{i',j',k'}$$

was used to obtain the values of ϕ outside the north-south boundaries. Where $u^*_{i',j',k'}$ represents the volume average of the u velocity field at the boundary. The results reported here were for the special case of $f_o = 0$. For this case, the boundary condition then becomes:

$$\left(\frac{\partial \phi}{\partial y}\right)_{i',j',k'} = 0 \quad .$$

Figure 2 illustrates the vertical grid domain and boundary placements. The top and bottom boundaries are set in manner similar to the north-south boundaries where the points midway between K = KM - 1 and K = KM - 2 and K = 2 and K = 3 are the top and bottom boundaries respectively. The no-flux condition is imposed on the w field by:

$$W_{I,J,1} = -W_{I,J,4}$$

$$W_{I,J,2} = -W_{I,J,3}$$

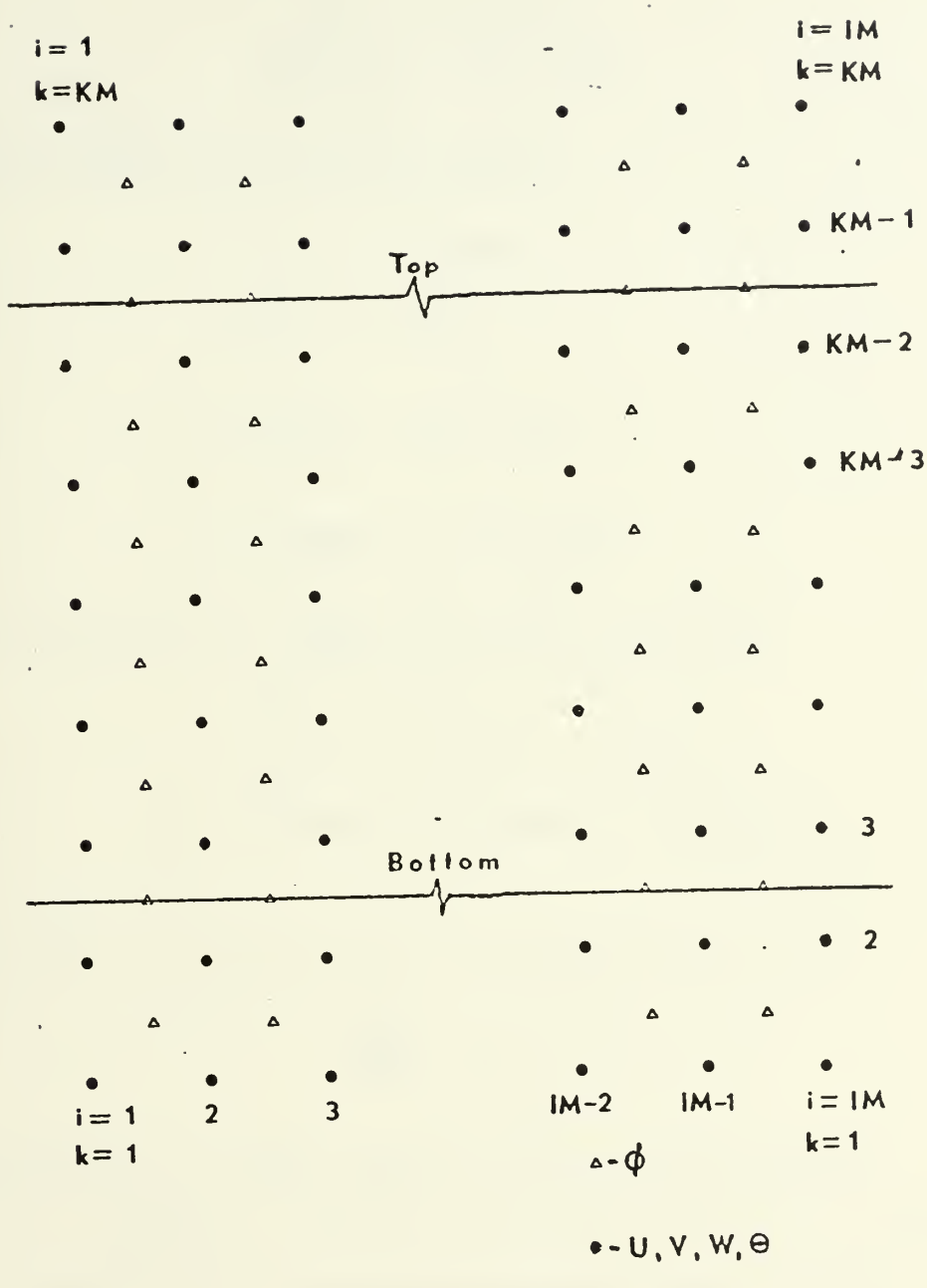

Figure 2. Illustration of the grid system in the vertical direction.

$$W_{I,J,KM} = -W_{I,J,KM-3}$$

$$W_{I,J,KM-1} = -W_{I,J,KM-2} \quad ,$$

while the θ values are set by the relations:

$$\theta_{I,J,1} = -\theta_{I,J,4}$$

$$\theta_{I,J,2} = -\theta_{I,J,3}$$

$$\theta_{I,J,KM} = -\theta_{I,J,KM-3}$$

$$\theta_{I,J,KM-1} = -\theta_{I,J,KM-2} \quad .$$

The values of u and v are simply extrapolated outward by:

$$S_{I,J,1} = S_{I,J,2} = S_{I,J,3}$$

$$S_{I,J,KM} = S_{I,J,KM-1} = S_{I,J,KM-2}$$

where S = u,v.

The value of the pressure term is obtained by the use of:

$$\left(\frac{\partial \phi}{\partial z}\right)_{i',j',k'} = 0 \quad .$$

The importance of proper boundary conditions cannot be over-emphasized. This model was found to be extremely sensitive to all the boundary conditions. The complete development of the boundary conditions is found in Appendix C.

V. INITIAL CONDITIONS

Initialization of the u,v,w and θ fields is accomplished by the use of linearized gravity wave solutions, which are exact for small amplitude gravity waves and are derived from the following equations:

$$\frac{\partial u}{\partial t} = - \frac{\partial \phi}{\partial x}$$

$$\frac{\partial v}{\partial t} = - \frac{\partial \phi}{\partial y}$$

$$\frac{\partial w}{\partial t} = - \frac{\partial \phi}{\partial z} + \frac{g\theta}{\theta_o}$$

$$\nabla_3 \cdot \bar{V} = 0$$

and

$$\frac{\partial \theta}{\partial t} = - w \frac{\partial \bar{\theta}}{\partial z} \quad .$$

The exact solutions for a stable wave propagating in the x direction are given by:

$$u = - \frac{\lambda m W}{\lambda^2 + \mu^2} \sin(\lambda x - ct) \cos \mu y \cos mz \quad ,$$

$$v = - \frac{\mu m W}{\lambda^2 + \mu^2} \cos(\lambda x - ct) \sin \mu y \cos mz \quad ,$$

$$w = W \cos(\lambda x - ct) \cos \mu y \sin mz \quad ,$$

$$\theta = \frac{W}{\lambda c} \frac{\partial \bar{\theta}}{\partial z} \sin(\lambda x - ct) \cos \mu y \sin mz \quad .$$

where c represents the phase speed of the stable gravity wave in m sec^{-1} and is calculated from:

$$c = \frac{N}{\lambda} \sqrt{\frac{\lambda^2 + \mu^2}{\lambda^2 + \mu^2 + m^2}} \qquad (15)$$

and N is the Brunt Väisälä frequency

$$N = \sqrt{\frac{g}{\theta_o} \frac{\partial \bar{\theta}}{\partial z}} \quad .$$

The initial guess for the ϕ field is chosen to be an arbitrary constant (2.0) due to the extremely efficient relaxation technique. The set of exact solutions with t = 0 was used to initialize the fields.

VI. RESULTS

By introducing a stable gravity wave perturbation into the basic model, the wave form can be tested for proper phase speed, amplitude growth or decay and computational stability. The initial conditions should result in a wave that propagates in the x direction alone with no growth in amplitude. Figures 3a, 3b, 3c, and 3d are representative plotted values of the u,v,w, and θ wave forms after time steps 10, 20, 30, and 40, with the initial value present for comparison. These plots are for the wave forms in the x direction for J = 5 and K = 7 and show the phase speed relationship between the various time steps. The exact solution to equation (15) yields a phase speed of 5.5 m sec^{-1} for the specified values W = .01 m sec^{-1} and N = 4.04 x 10^{-3} sec^{-1}. Phase speed calculated from the plotted values is 5.4 m sec^{-1} for each of the four wave forms. There is negligible amplitude growth or decay in any of the plots.

Figures 4a, 4b, 4c, and 4d are the plotted values of the wave forms in the y direction for I = 5 and K = 7. The plots indicate there is no propagation in the y direction. Due to the nature of the solutions to the linearized equations, the wave forms should oscillate about the zero value as indicated in the stated figures.

Plots of the wave forms in the z direction for I = 5 and J = 5 are shown in Figures 5a, 5b, 5c, and 5d and are similar in amplitude oscillation to the y direction with no phase speed observed.

The main objective of this staggered grid model was to reduce the storage size and computer time required for an operational small scale convective model. The previous full-grid model required 502K bytes of

storage and approximately 20 minutes of computer time to produce a 40 time step forecast. The forecasts produced by the staggered grid model accomplishes a 40 time step prognosis in less than 10 minutes of computer time and requires only 156K bytes of storage.

The results obtained after 40 time steps compared to the analytical solutions illustrate the accuracy of the finite difference solutions. However, a few time steps later, the solutions fail to converge. A further discussion of this difficulty will be given in a later section.

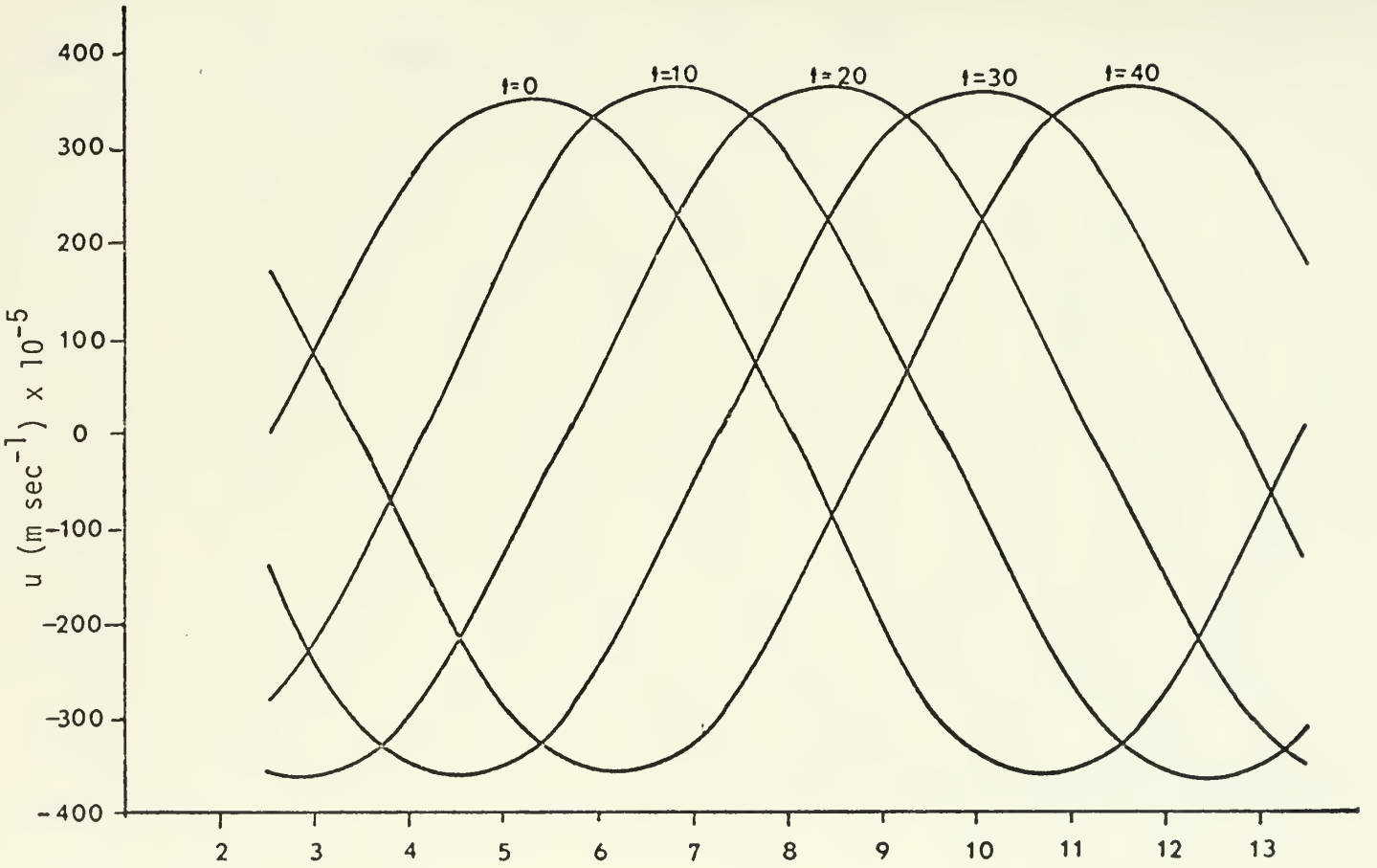

Figure 3a. u component of stable gravity wave in x direction for J = 5, K = 7.

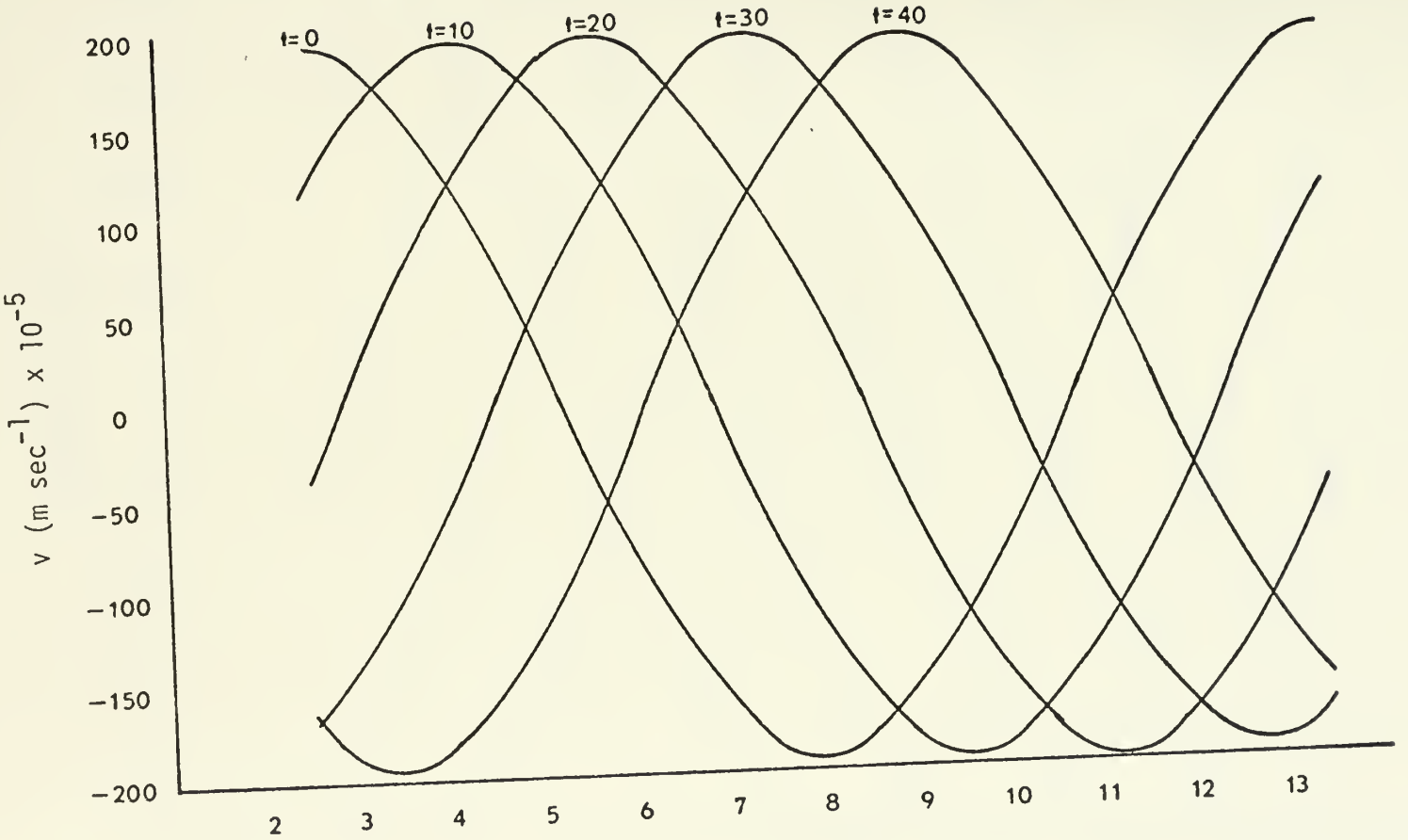

Figure 3b. v component of stable gravity wave in x direction for J = 5, K = 7.

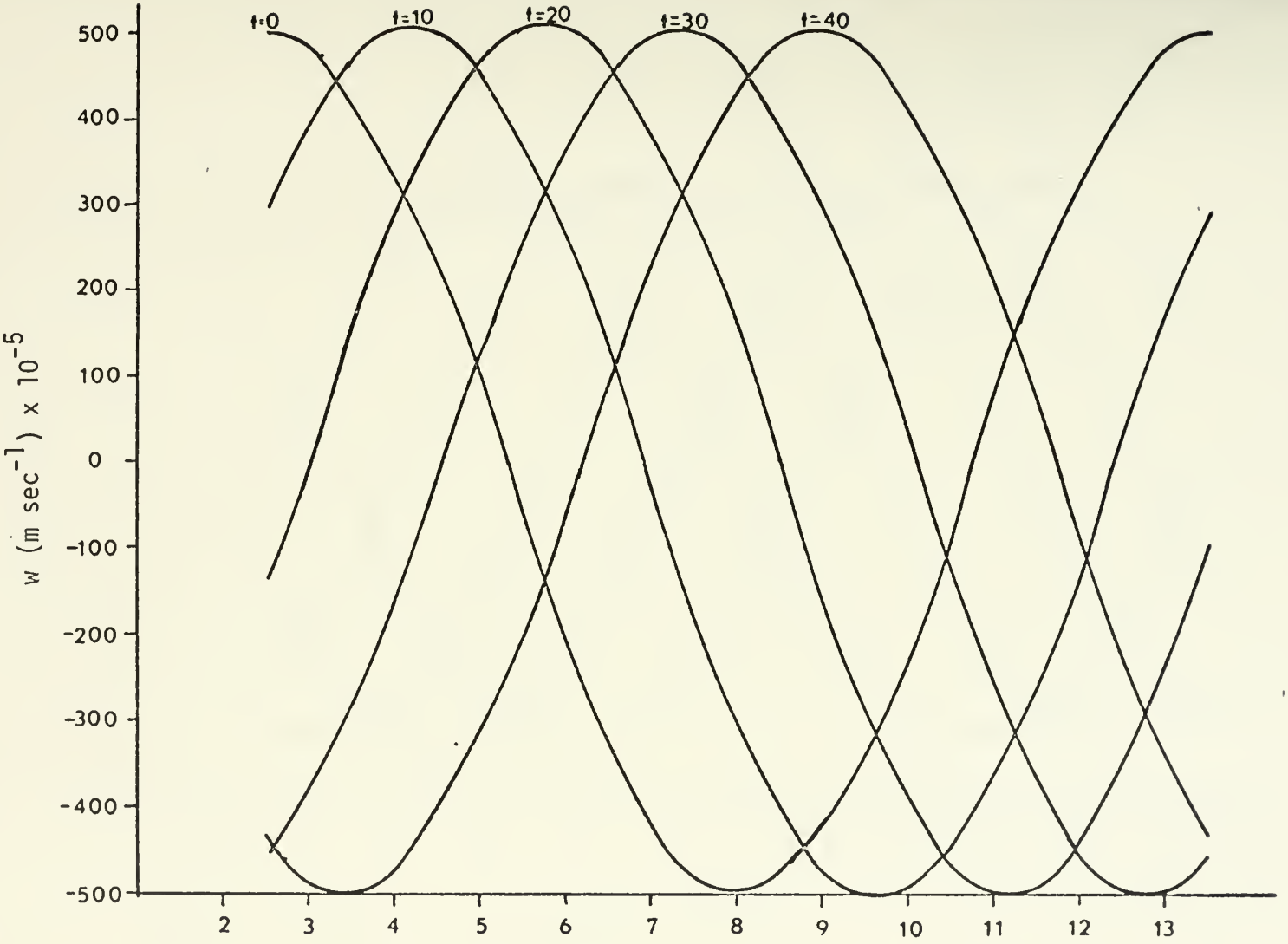

Figure 3c. w component of stable gravity wave in x direction for J = 5, K = 7.

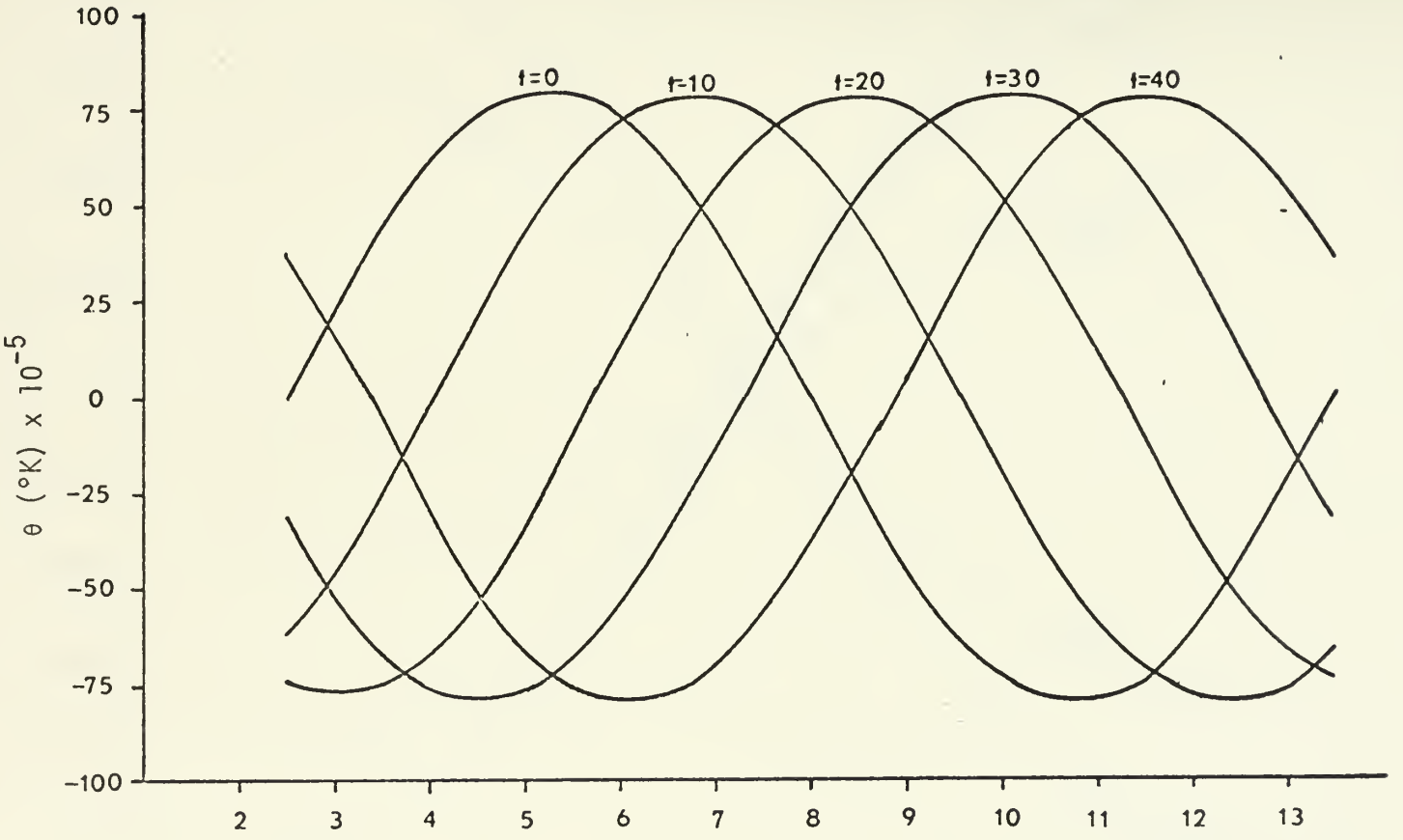

Figure 3d. θ wave in x direction for J = 5, K = 7.

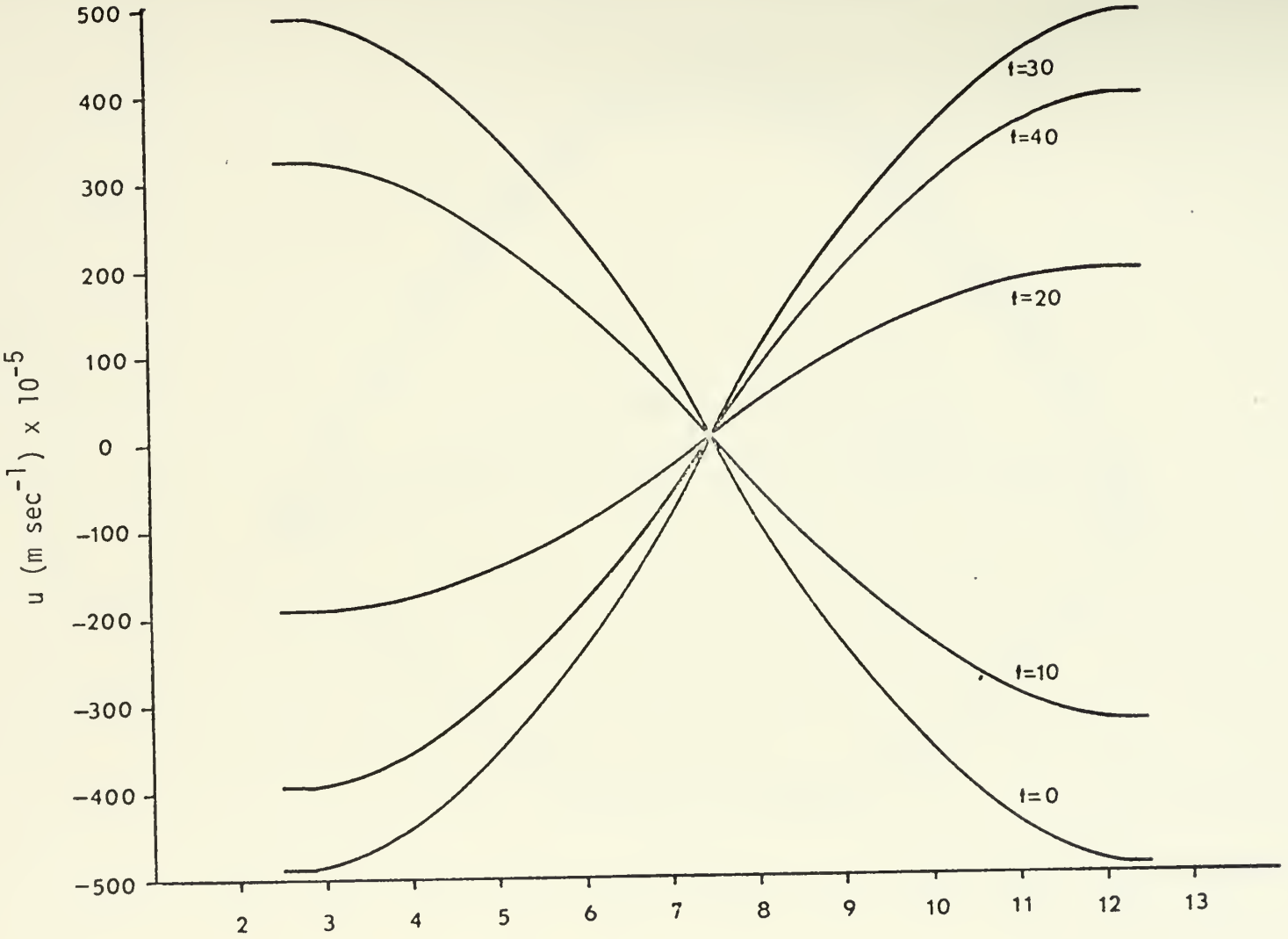

Figure 4a. u component of stable gravity wave in y direction for I = 5, K = 7.

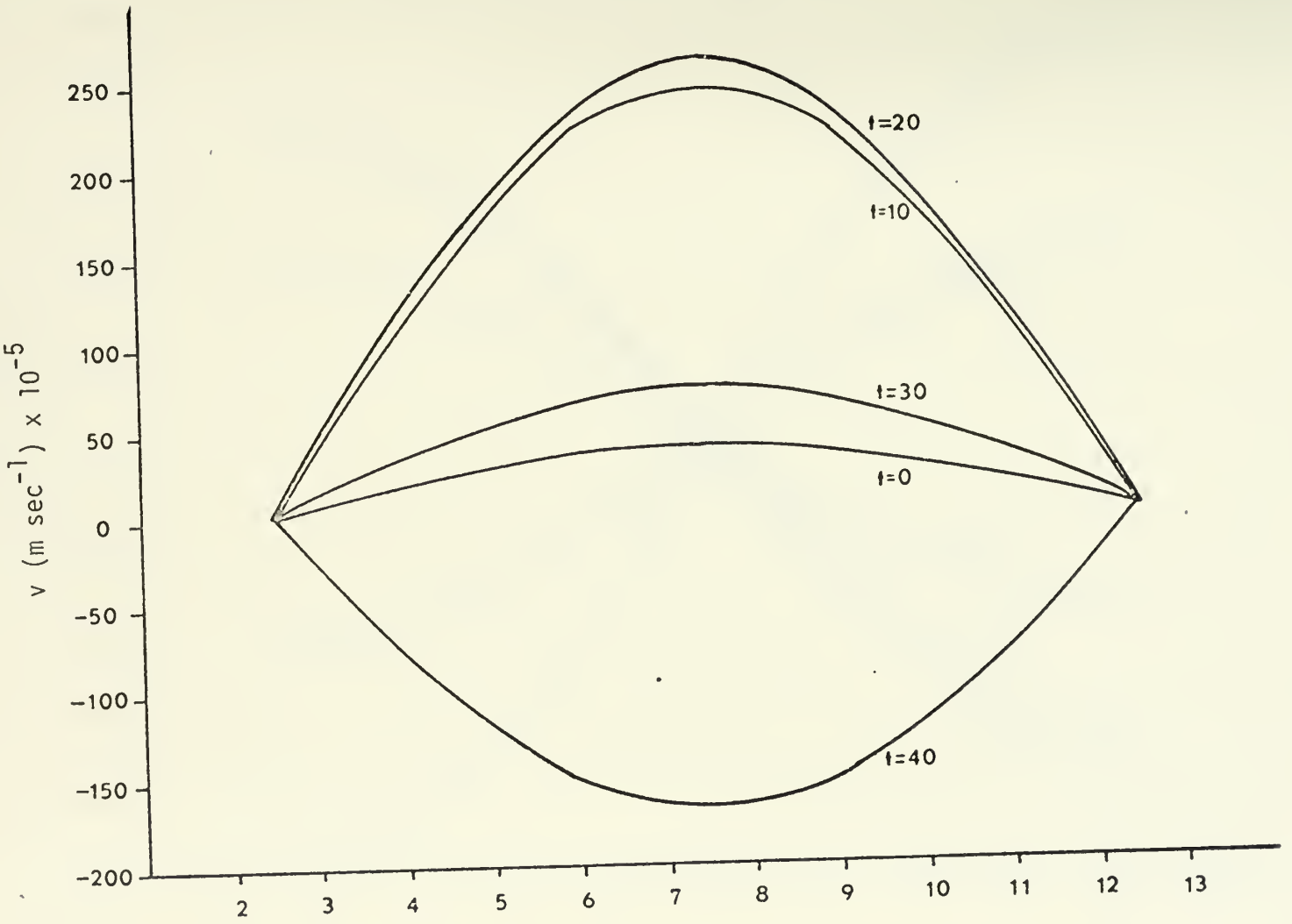

Figure 4b. v component of stable gravity wave in y direction for I = 5, K = 7.

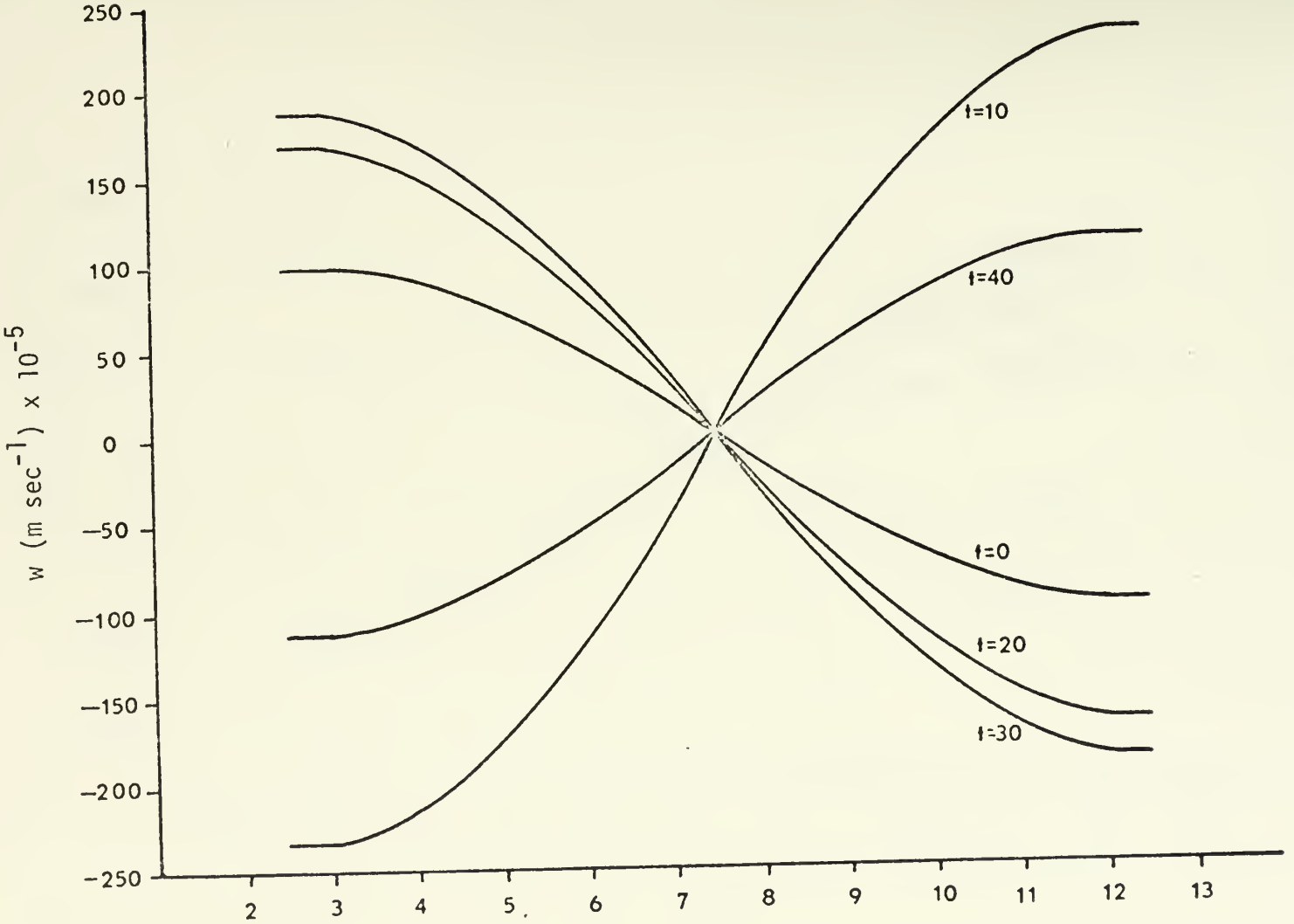

Figure 4c. w component of stable gravity wave in y direction for I = 5, K = 7.

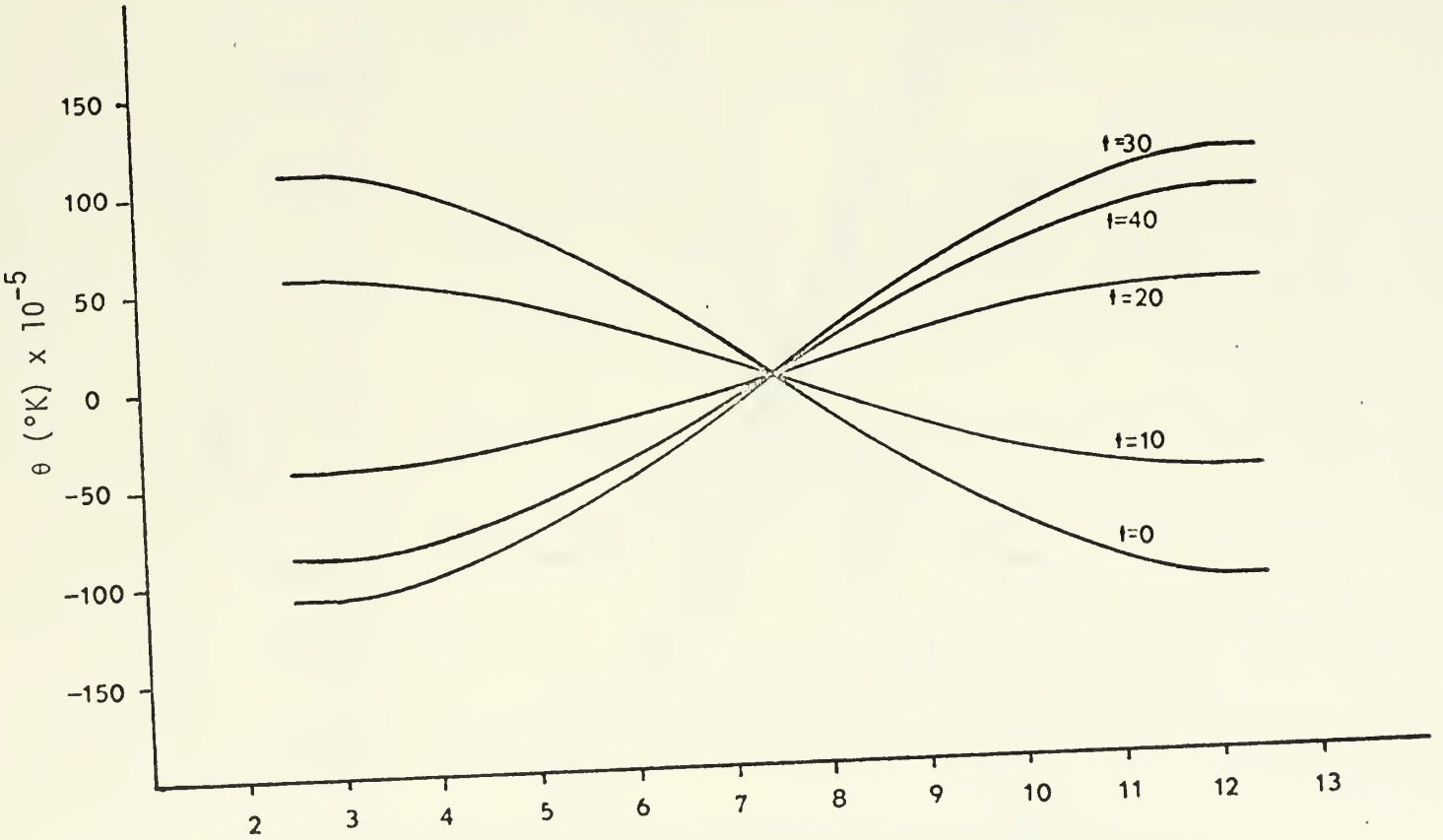

Figure 4d. θ wave in the y direction for I = 5, K = 7.

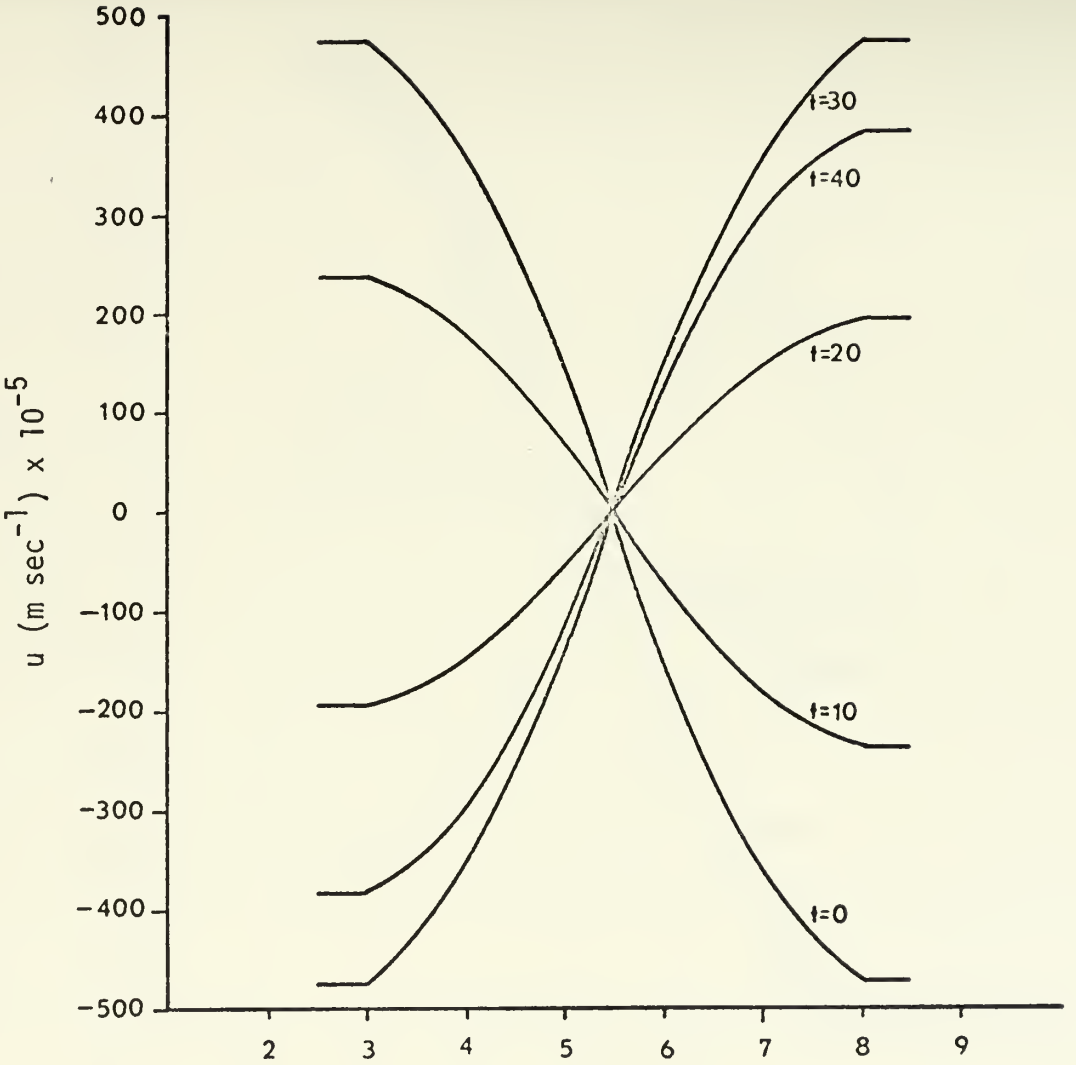

Figure 5a. u component of stable gravity wave in z direction for I = 5, J = 5.

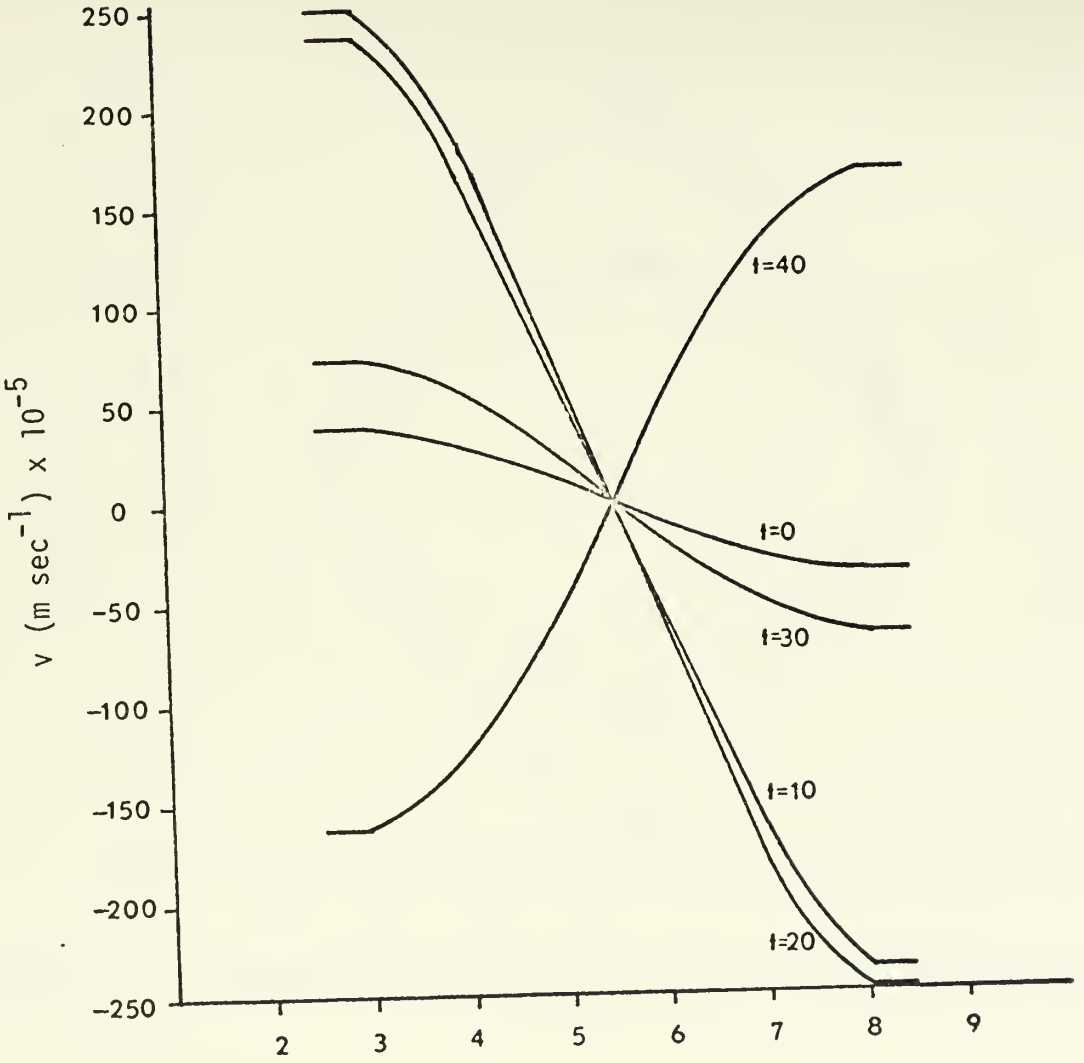

Figure 5b. v component of stable gravity wave in z direction for I = 5, J = 5.

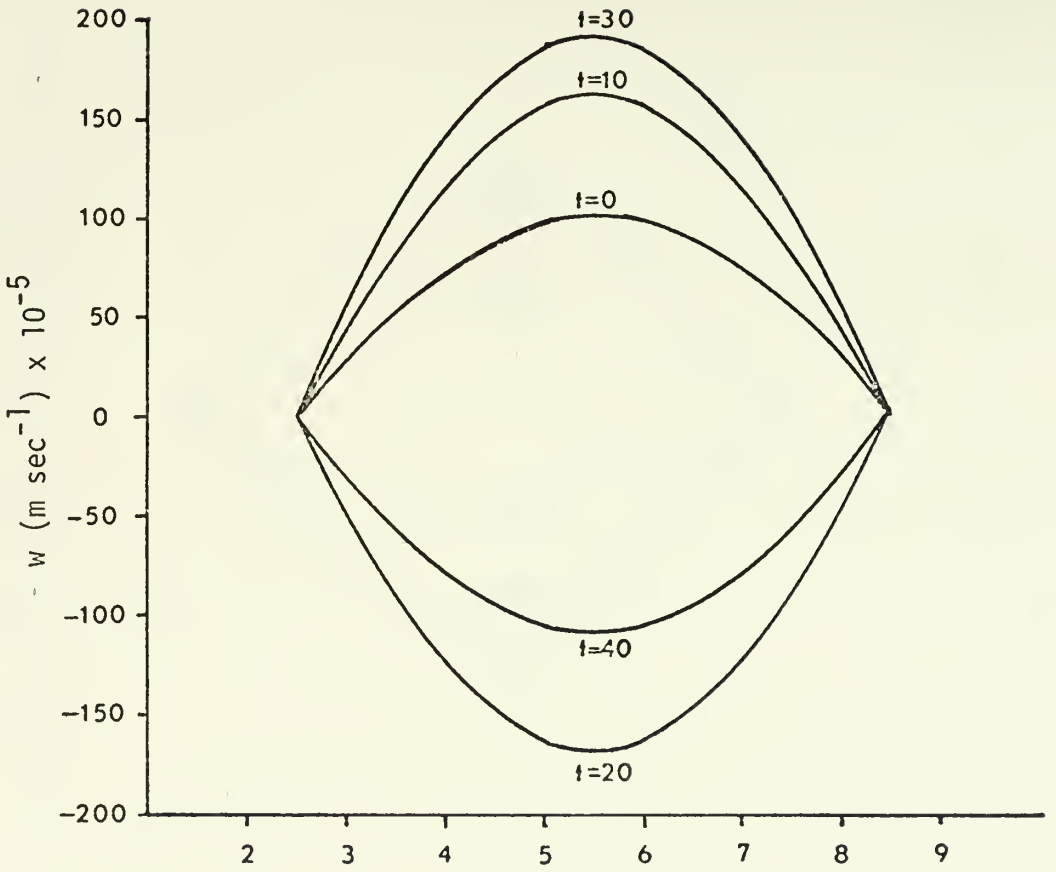

Figure 5c. w component of stable gravity wave in z direction for I = 5, J = 5.

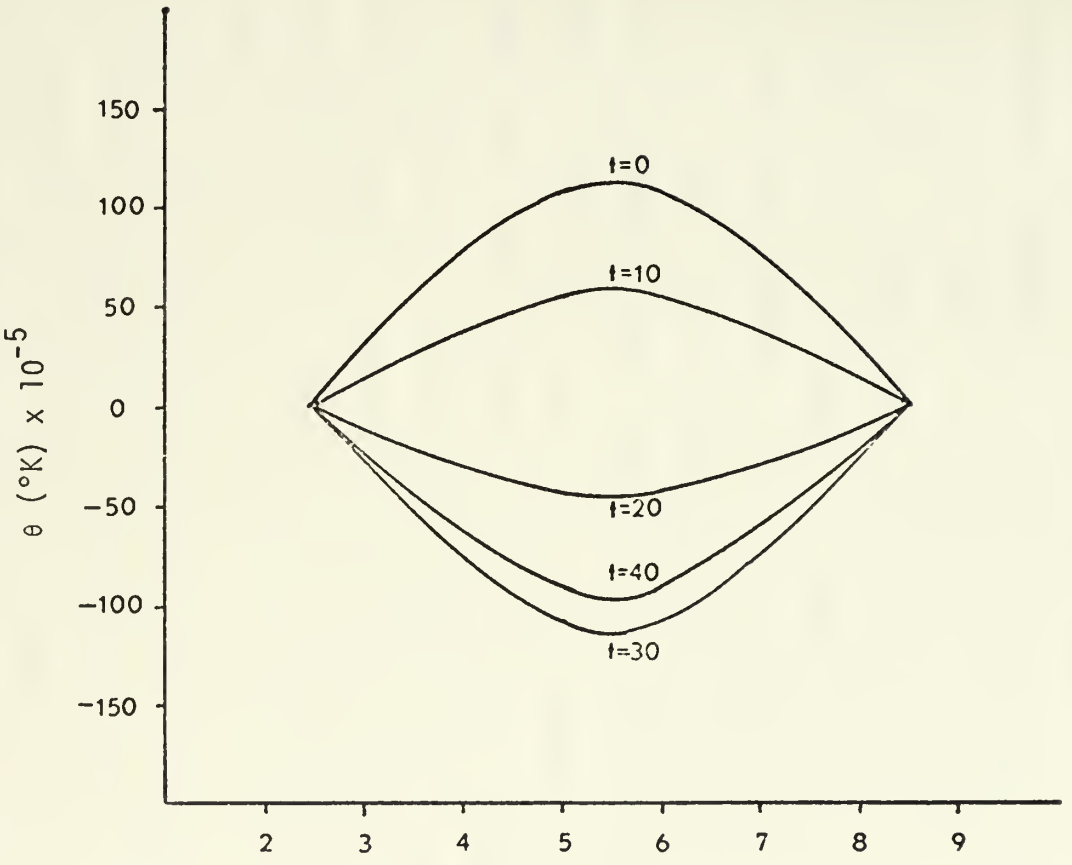

Figure 5d. θ wave in z direction for I = 5, J = 5.

VII. CONCLUSIONS AND SUMMARY

A ten-level staggered grid primitive equation model was applied to a mesoscale grid and tested with an initial stable gravity wave perturbation to check the computational stability and finite difference form of the equations of motion. Comparing the results presented here to a non-staggered grid model, the computer time and storage requirements have been reduced to about 1/3 of the full grid model.

The forecasts produced by this model compare quite closely with the full grid model but ceases to function after 47 time steps. Up until this time step all fields appear to be predicted properly. Tests were run in double precision to determine if truncation error was a problem and the same type of results occured with the model failing to converge after 47 time steps. In all cases the points that failed to converge were near the boundaries which leads to the conclusion that further refinements of the boundary conditions may be necessary. Experiments have shown that a less stringent relaxation tolerance produces less exact ϕ gradients which in turn induces greater errors in the prognosis of the other parameters. Apparently there is still some difficulty in the program and presently studies are being co.ducted to further refine this model.

Continued studies using this model should have a provision for including vertical compressibility. Additionally, since a primary source of the energy in a thunderstorm-type cloud is latent heat, application to cumulus scale convective activity would be inadequate without the inclusion of moisture.

APPENDIX A

EXTRAPOLATED LIEBMANN RELAXATION SCHEME

FOR THREE DIMENSIONAL APPLICATION

The equation to be solved by relaxation is:

$$\nabla^2\phi - F = 0 \qquad \text{(A-1)}$$

where the tendency of the divergence is zero and:

$$F = -\nabla_3 \cdot \left[(\bar{V}_3 \cdot \nabla_3)\bar{V}_3\right] + f_o\,\zeta + \frac{g}{\theta_o}\,\frac{\partial\theta}{\partial z} \quad . \qquad \text{(A-2)}$$

with the ϕ points staggered in the vertical as well as in the horizontal. (They are located one-half grid distance above or below the diagonals connecting velocity points as in Fig. A1.) In other words, the velocity and θ points are located at the corners of a cube and the ϕ point in the center. For convenience, a new temporary indexing scheme will be utilized by writing:

$$i' = i - \frac{1}{2}$$

$$j' = j - \frac{1}{2}$$

$$k' = k - \frac{1}{2}$$

where i,j,k represent u,v,w and θ points and i', j', k' represent ϕ points. Writing (A-1) with this new notation in finite difference form at the point i', j', k' and expanding yields:

$$\frac{1}{(4\Delta x)^2}\Big[\phi_{i'+1,j'+1,k'+1} + 2\phi_{i'+1,j',k'+1} + \phi_{i'+1,j'-1,k'+1} - 2\phi_{i',j+1,k'+1}$$

$$-4\phi_{i',j',k'+1} - 2\phi_{i',j'-1,k'+1} + \phi_{i'-1,j'+1,k'+1} + 2\phi_{i'-1,j',k'+1}$$

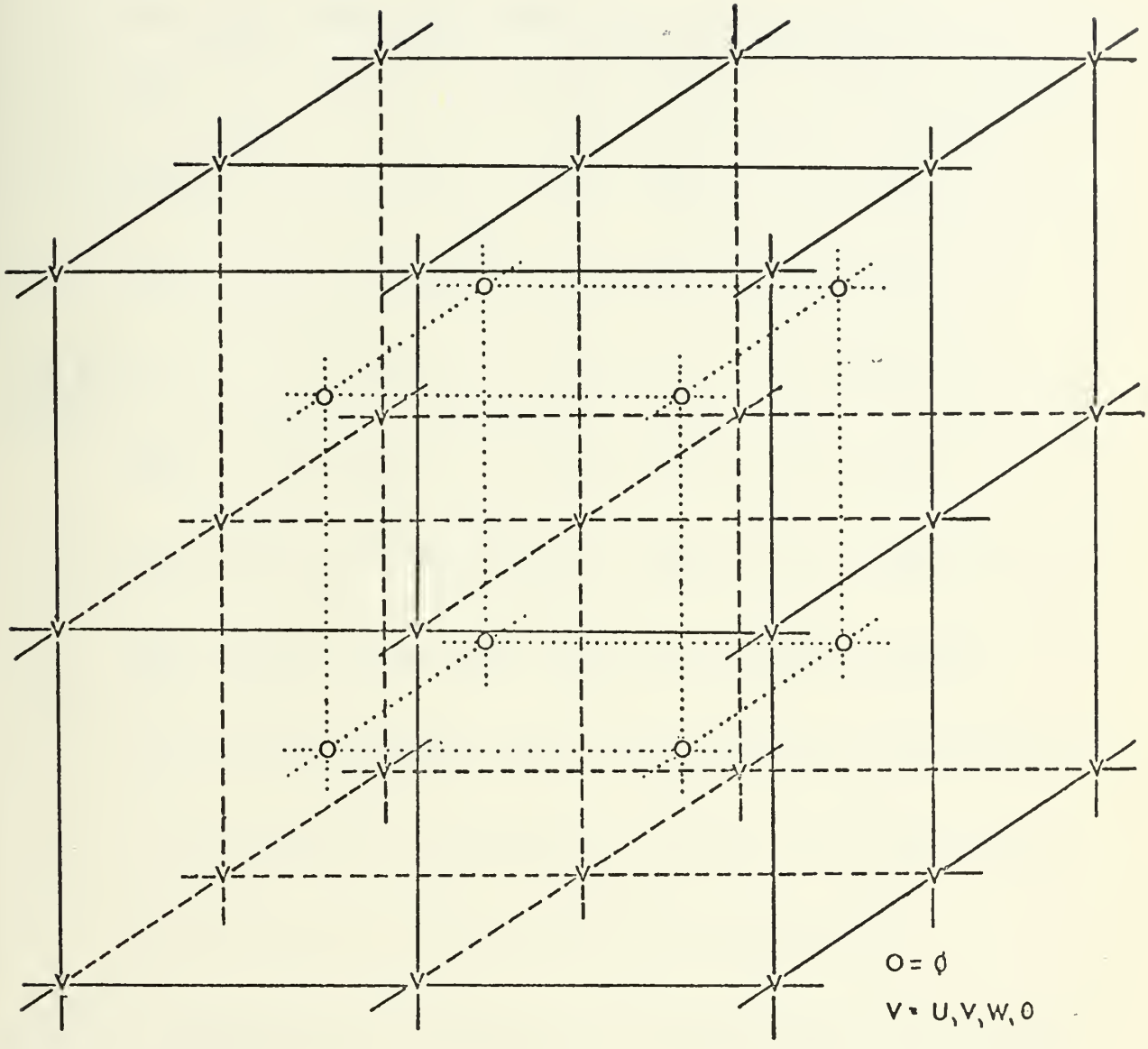

Figure A1. Three dimensional schematic of the location of Various fields.

$$+\phi_{i'-1,j'-1,k'+1} + 2\phi_{i'+1,j'+1,k'} + 4_{i'+1j',k'} + 2\phi_{i'+1,j'-1,k'}$$

$$-4\phi_{i',j+1,k'} - 8\phi_{i',j',k'} - 4\phi_{i',j-1,k'} + 2\phi_{i'-1,j'+1,k'}$$

$$+4\phi_{i'-1,j',k'} + 2\phi_{i'-1,j'-1,k'} + \phi_{i'+1,j'+1,k'-1} + 2\phi_{i'+1,j',k'-1}$$

$$+\phi_{i'+1,j'-1,k'-1} - 2\phi_{i',j'+1,k'-1} - 4\phi_{i',j',k'-1} - 2\phi_{i',j'-1,k'-1}$$

$$+\phi_{i'-1,j'+1,k'-1} + 2\phi_{i'-1,j',k'-1} + \phi_{i'-1,j'-1,k'-1}\Big] +$$

$$\frac{1}{(4\Delta y)^2}\Big[\phi_{i'+1,j'+1,k'+1} - 2\phi_{i'+1,j,k'+1} + \phi_{i'+1,j'-1,k'+1} + 2\phi_{i',j'+1,k'+1}$$

$$-4\phi_{i',j',k'+1} + 2\phi_{i',j'-1,k'+1} + \phi_{i'-1,j'+1,k'+1} - 2\phi_{i'-1,j',k'+1}$$

$$+\phi_{i'-1,j'-1,k'+1} + 2\phi_{i'+1,j'+1,k'} - 4\phi_{i'+1,j',k'} + 2\phi_{i'+1,j'-1,k'}$$

$$+4\phi_{i',j'+1,k'} - 8\phi_{i',j',k'} + 4\phi_{i',j'-1,k'} + 2\phi_{i'-1,j'+1,k'}$$

$$-4\phi_{i'-1,j',k'} + 2\phi_{i'-1,j'-1,k'} + \phi_{i'+1,j'+1,k'-1} - 2\phi_{i'+1,j',k'-1}$$

$$+\phi_{i'+1,j'-1,k'-1} + 2\phi_{i',j'+1,k'-1} - 4\phi_{i',j',k'-1} + 2\phi_{i',j'-1,k'-1}$$

$$+\phi_{i'-1,j'+1,k'-1} - 2\phi_{i'-1,j',k'-1} + \phi_{i'-1,j'-1,k'-1}\Big] +$$

$$\frac{1}{(4\Delta z)^2}\Big[\phi_{i'+1,j'+1,k'+1} + 2\phi_{i'+1,j'k'+1} + \phi_{i'+1,j'-1,k'+1} + 2\phi_{i',j'+1,k'+1}$$

$$+4\phi_{i',j',k'+1} + 2\phi_{i',j'-1,k'+1} + \phi_{i'-1,j'+1,k'+1} + 2\phi_{i'-1,j',k'+1}$$

$$+\phi_{i'-1,j'-1,k'+1} - 2\phi_{i'+1,j'+1,k'} - 4\phi_{i'+1,j',k'} - 2\phi_{i'+1,j'-1,k'}$$

$$-4\phi_{i',j'+1,k'} - 8\phi_{i',j',k'} - 4\phi_{i',j'-1,k'} - 2\phi_{i'-1,j'+1,k'}$$

$$-4\phi_{i'-1,j',k'} - 2\phi_{i'-1,j'-1,k'} + \phi_{i'+1,j'+1,k'-1} + 2\phi_{i'+1,j',k'-1}$$

$$+\phi_{i'+1,j'-1,k'-1} + 2\phi_{i',j'+1,k'-1} + 4\phi_{i',j',k'-1} + 2\phi_{i',j'-1,k'-1}$$

$$+\phi_{i'-1,j'+1,k'-1} + 2\phi_{i'-1,j',k'-1} + \phi_{i'-1,j'-1,k'-1}\Big] - F_{i',j',k'} = 0 \qquad \text{(A-3)}$$

Rearranging terms and clearing fractions leads to:

$$(4\Delta y)^2 (4\Delta z)^2 \left[B - 8\phi_{i',j',k'}\right]$$

$$+(4\Delta x)^2 (4\Delta z)^2 \left[C - 8\phi_{i',j',k'}\right]$$

$$+(4\Delta x)^2 (4\Delta y)^2 \left[D - 8\phi_{i',j',k'}\right]$$

$$-(4\Delta x)^2 (4\Delta y)^2 (4\Delta z)^2 F_{i',j',k'} = 0 \qquad \text{(A-4)}$$

where B, C and D represent the finite difference forms in equation (A-3) with the term $8\phi_{i',j',k'}$ subtracted off. With further rearranging of terms (A-4) becomes:

$$\phi_{i',j',k'} = A\Big[(4\Delta y)^2 (4\Delta z)^2 B + (4\Delta x)^2 (4\Delta z)^2 C + (4\Delta x)^2 (4\Delta y)^2 D - (4\Delta x)^2 (4\Delta y)^2 (4\Delta z)^2 F_{i',j',k'}\Big]$$

where:

$$A = \frac{1}{8\left[(4\Delta y)^2 (4\Delta z)^2 + (4\Delta x)^2 (4\Delta z)^2 + (4\Delta x)^2 (4\Delta y)^2\right]} .$$

Adding and subtracting $\phi^{old}_{i',j',k'}$ yields:

$$\phi^{new}_{i',j',k'} = \phi^{old}_{i',j',k'} + \alpha A\Big[(4\Delta y)^2 (4\Delta z)^2 B + (4\Delta x)^2 (4\Delta z)^2 C + (4\Delta x)^2 (4\Delta y)^2 D - (4\Delta x)^2 (4\Delta y)^2 (4\Delta z)^2 F_{i',j',k'}\Big] . \qquad \text{(A-5)}$$

Where the over-relaxation coefficient α is introduced. (A-5) then becomes:

$$\phi^{new}_{i',j',k'} = (1 - \alpha)\, \phi^{old}_{i',j',k'} + \alpha A \Big[(4\Delta y)^2 (4\Delta z)^2 B + (4\Delta x)^2 (4\Delta z)^2 C + (4\Delta x)^2 (4\Delta y)^2 D - (4\Delta x)^2 (4\Delta y)^2 (4\Delta z)^2 F_{i',j',k'} \Big] . \qquad \text{(A-6)}$$

This was the form used for relaxation in the model. Many tests were run to determine the most efficient relaxation coefficient for this type of finite difference scheme. The value of α which resulted in the most efficient relaxation was 1.05. Note that if $\Delta x = \Delta y = \Delta z$, equation (A-6) reduces to the more familiar form:

$$\phi^{new}_{i',j',k'} = (1 - \alpha)\, \phi^{old}_{i',j',k'} + \frac{\alpha}{24} \Big[B + C + D - (4\Delta z)^2 F_{i',j',k'} \Big] .$$

The stencil of the method of the ∇^2 operator in the three dimensional staggered grid, assuming that the three grid lengths are equal, is shown in Fig. A2.

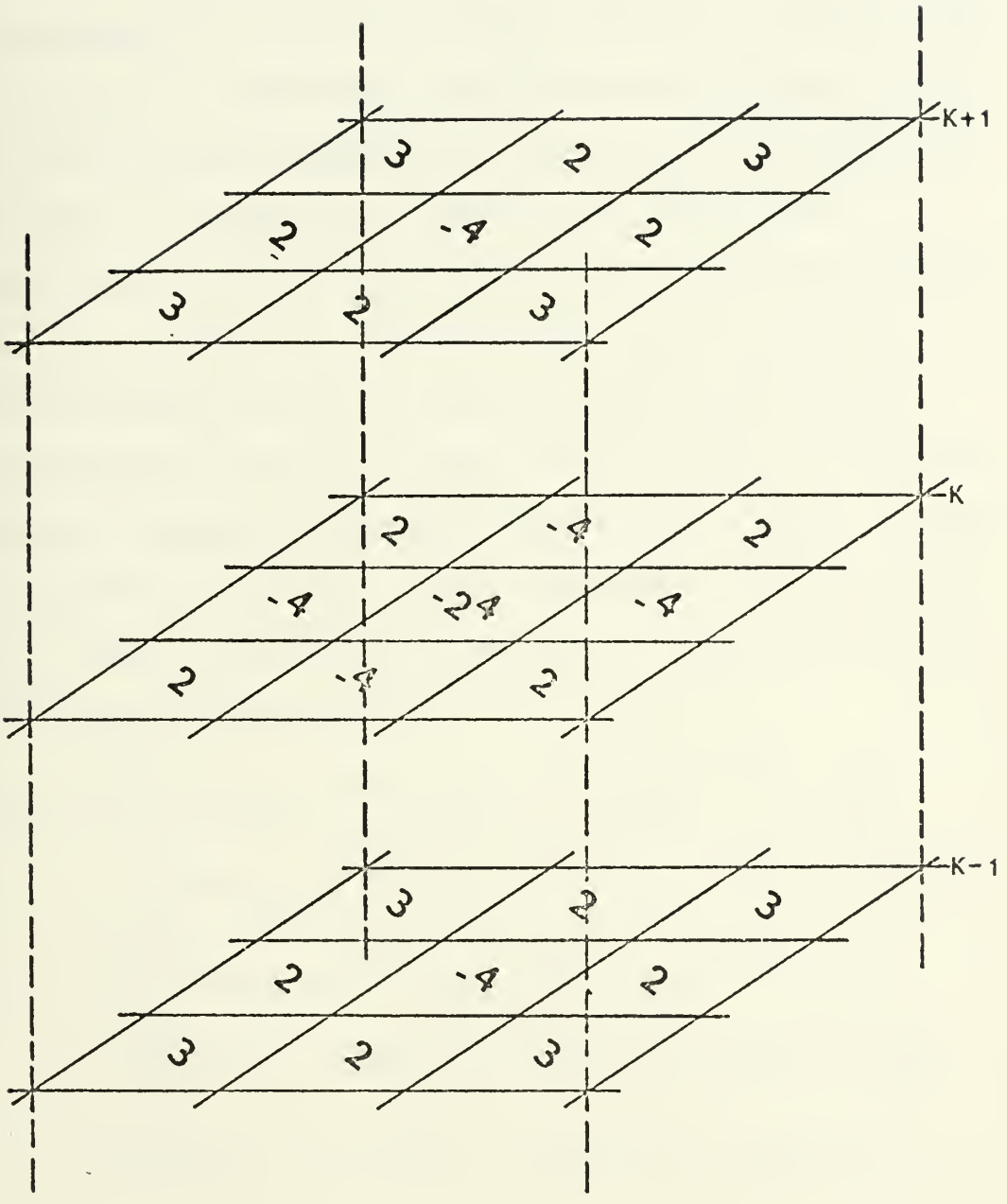

Figure A2. ψ^2 Operator in three dimensional form assuming $\Delta x = \Delta y = \Delta z$.

APPENDIX B

DEVELOPMENT OF THE FORCING FUNCTION

The formation of the forcing function used in the relaxation scheme is a long process. Consistency between the finite difference methods used in the prognostic equations and in the relaxation technique must be maintained. The computation of the forcing function given in equation (A-2) in finite difference form follows. In order to determine this forcing function in a consistent manner, the forcing function must first be calculated at an i,j,k point and then volume averaged to have the function at an i',j',k' point. Each of the three directional components are computed separately and then summed to put the complete forcing function at the desired point. For example, in order to form $F_{5',5',5'}$ (the forcing function at the point i' = 5, j' = 5, k' = 5) the following steps are required:

$$F^{x}_{5',5',5'} = \left\{ \frac{1}{4} \left[G(u)_{6,6,6} + G(u)_{6,5,6} + G(u)_{6,6,5} + G(u)_{6,5,5} \right] - \frac{1}{4} \left[G(u)_{5,6,6} + G(u)_{5,5,6} + G(u)_{5,6,5} + G(u)_{5,5,5} \right] \right\} \frac{1}{\Delta x}$$

$$F^{y}_{5',5',5'} = \left\{ \frac{1}{4} \left[G(v)_{6,6,6} + G(v)_{5,6,6} + G(v)_{6,6,5} + G(v)_{5,6,5} \right] - \frac{1}{4} \left[G(v)_{6,5,6} + G(v)_{5,5,6} + G(v)_{6,5,5} + G(V)_{5,5,5} \right] \right\} \frac{1}{\Delta y}$$

$$F^{z}_{5',5',5'} = \left\{ \frac{1}{4} \left[G(w)_{6,6,6} + G(w)_{6,5,6} + G(w)_{5,6,6} + G(w)_{5,5,6} \right] - \frac{1}{4} \left[G(w)_{6,6,5} + G(w)_{6,5,5} + G(w)_{5,6,5} + G(w)_{5,5,5} \right] \right\} \frac{1}{\Delta z}$$

$$F_{5',5',5'} = F^{x}_{5',5',5'} + F^{y}_{5',5',5'} + F^{z}_{5',5',5}$$

where

$$G(u) = - L(u) + fv + \nu\nabla_3^2 u \quad ,$$

$$G(v) = - L(v) - fu + \nu\nabla_3^2 v \quad ,$$

$$G(w) = - L(w) + \frac{g\theta}{\theta_o} + \nu\nabla_3^2 w \quad .$$

and the G functions are calculated on the i,j,k grid.

APPENDIX C

COMPLETE DEVELOPMENT OF THE BOUNDARY CONDITIONS

For the boundary described by the plane of $j' = 2\frac{1}{2}$, the y component of the equation of motion may be written

$$\frac{\partial v}{\partial t}_{i',2,k'} = 0$$

which implies

$$\frac{\partial v}{\partial t}_{i,3,k} = - \frac{\partial v}{\partial t}_{i,2,k} \qquad \text{(C-1)}$$

Further expansion of each of the terms leads to:

$$\frac{\partial v}{\partial t}_{i,3,k} = - L(v)_{i,3,k} - \frac{\partial \phi}{\partial y}_{i,3,k} - f_o u_{i,3,k} \qquad \text{(C-2}$$

and

$$- \frac{\partial v}{\partial t}_{i,2,k} = L(v)_{i,2,k} + \frac{\partial \phi}{\partial y}_{i,2,k} + f_o u_{i,2,k} \qquad \text{(C-3)}$$

By introducing the no-flux conditions on v at the lateral walls from (C-1), (C-2) and (C-3) yield:

$$- \frac{\partial \phi}{\partial y}_{i,3,k} - f_o u_{i,3,k} = \frac{\partial \phi}{\partial y}_{i,2,k} + f_o u_{i,2,k} \qquad \text{(C-4)}$$

Expansion of (C-4) into finite differences and averaging the u field to be consistent with the ϕ field yields:

$$\phi_{i',1,k'} = \phi_{i',3,k'} + \frac{\Delta y f_o}{2} \left(u_{i,2,k} + u_{i+1,2,k} + u_{i,2,k+1} + u_{i+1,2,k+1}\right)$$

with the no-flux conditions being:

$$v_{i,2,k} = -v_{i,3,k}$$

$$v_{i,1,k} = -v_{i,4,k}$$

A similar approach is taken at the northern boundary with the following conditions:

$$v_{i,J1,k} = -v_{i,J2,k}$$

$$v_{i,JM,k} = -v_{i,J3,k}$$

$$\phi_{i',J1,k'} = \phi_{i',J3,k'} - \frac{\Delta y f_o}{2} (u_{i,J2,k} + u_{i+1,J2,k}$$

$$+u_{i,J2,k+1} + u_{i+1,J2,k+1}) \quad .$$

The case considered here was for $f_o = 0$.

For the boundary described by k' = 2', the z component of the equation of motion may be written:

$$\frac{\partial w}{\partial t}_{i',2',k'} = 0$$

which implies:

$$\frac{\partial w}{\partial t}_{i,3,k} = - \frac{\partial w}{\partial t}_{i,2,k} \qquad \text{(C-5)}$$

Further expansion of each of the terms in (C-5) yields:

$$\frac{\partial w}{\partial t}_{i,3,k} = - L(w)_{i,3,k} - \frac{\partial \phi}{\partial z}_{i,3,k} + \frac{g}{\theta_o} \theta_{i,3,k} \qquad \text{(C-6)}$$

$$- \frac{\partial w}{\partial t}_{i,2,k} = + L(w)_{i,2,k} + \frac{\partial \phi}{\partial z}_{i,2,k} - \frac{g}{\theta_o} \theta_{i,2,k} \quad . \qquad \text{(C-7)}$$

By introducing the no-flux conditions on w at the top and bottom boundaries from (C-5), (C-6) and (C-7) they yield:

$$- \frac{\partial \phi}{\partial z}_{i,3,k} + \frac{g}{\theta_o} \theta_{i,3,k} = \frac{\partial \phi}{\partial z}_{i,2,k} - \frac{g}{\theta_o} \theta_{i,2,k} \qquad \text{(C-8)}$$

By setting θ at the boundaries as previously discussed, (C-8) is satisfied if:

$$\phi_{i',j',1'} = \phi_{i',j',3'}$$

where the θ boundary conditions are:

$$\theta_{i,j,2} = - \theta_{i,j,3}$$

$$\theta_{i,j,1} = - \theta_{i,j,4} \quad .$$

A similar approach is taken at the top boundary with the following conditions:

$$\theta_{i,j,K1} = -\theta_{i,j,K2}$$

$$\theta_{i,j,KM} = -\theta_{i,j,K3}$$

and

$$\theta_{i',j',K1'} = \theta_{i',j',K3'} \quad .$$

LIST OF REFERENCES

1. Arakawa, A., 1962, "Non-geostrophic Effects in the Baroclinic Prognostic Equations". Proc. Intern, Symp. Numerical Weather Prediction, Tokyo, pp. 161-175.

2. Deardorff, J.W., 1970, "A Numerical Study of Three Dimensional Turbulent Channel Flow at Large Reynolds Numbers", J. Fluid Mech., 41, pp. 453-480.

3. Matsumoto, S., and K. Ninomiya, 1969, "On the Role of Convective Momentum Exchange in the Mesoscale Gravity Wave", J. Meteor. Soc. Japan, 47, no. 2, pp. 75-85

4. Norton, J.R., 1970, A Three Dimensional Primitive Equation Model for Application to Mesoscale Atmosphere Phenomena, M.S. Thesis, Naval Postgraduate School, Monterey, California.

5. Ogura, Y., 1963, "A Review of Numerical Modeling Research on Small Scale Convection in the Atmosphere", Meteorological Monographs, 5, pp. 65-76.

6. Ogura, Y., and N.A. Phillips, 1962, "Scale Analysis of Deep and Shallow Convection in the Atmosphere. J. Atmos. Sci., 19. pp. 173-179.

7. Orszag, Steven A., 1969, "Numerical Methods for the Simulation of Turbulence", Phys. Fluid Mech., Supp. II, pp. 250-257.

8. Ukaji, K. and T. Matsuno, 1970, "Effect of Lateral Walls on the Onset of Convective Motions", J. Meteor. Soc. Japan, 48, no. 3, pp. 217-222.

INITIAL DISTRIBUTION LIST

		No. Copies
1.	Defense Documentation Center Cameron Station Alexandria, Virginia 22314	2
2.	Library, Code 0212 Naval Postgraduate School Monterey, California 93940	2
3.	Department of Meteorology Naval Postgraduate School Monterey, California 93940	1
4.	Asst Professor R.L. Alberty, Code 51 Al Department of Meteorology Naval Postgraduate School Monterey, California 93940	5
5.	Lt Robert Bozich OC Division USS John F. Kennedy CVA-67 FPO New York, New York 09501	2
6.	Asst Professor R.L. Elsberry, Code 51 Es Department of Meteorology Naval Postgraduate School Monterey, California 93940	1
7.	Professor G.J. Haltiner, Department Chairman Department of Meteorology Naval Postgraduate School Monterey, California 93940	1
8.	Naval Weather Service Command Naval Weather Service Headquarters Washington Navy Yard Washington, D.C. 20390	1
9.	Assoc Professor R.T. Williams, Code 51 Wu Department of Meteorology Naval Postgraduate School Monterey, California 93940	1
10.	Asst Professor Robert Haney Code 51 Hy Department of Meteorology Naval Postgraduate School Monterey, California 93940	1

Security Classification

DOCUMENT CONTROL DATA - R & D

(Security classification of title, body of abstract and indexing annotation must be entered when the overall report is classified)

ORIGINATING ACTIVITY (Corporate author)	2a. REPORT SECURITY CLASSIFICATION
Naval Postgraduate School Monterey, California 93940	Unclassified
	2b. GROUP

REPORT TITLE

A Three Dimensional Staggered Grid Primitive Equation Model for Application to Mesoscale Atmospheric Motions

DESCRIPTIVE NOTES *(Type of report and, inclusive dates)*

Master's Thesis; March 1972

AUTHOR(S) *(First name, middle initial, last name)*

Robert Bozich

REPORT DATE	7a. TOTAL NO. OF PAGES	7b. NO. OF REFS
March 1972	51	8

CONTRACT OR GRANT NO.	9a. ORIGINATOR'S REPORT NUMBER(S)
PROJECT NO.	
	9b. OTHER REPORT NO(S) *(Any other numbers that may be assigned this report)*

DISTRIBUTION STATEMENT

Approved for public release; distribution unlimited.

SUPPLEMENTARY NOTES	12. SPONSORING MILITARY ACTIVITY
	Naval Postgraduate School Monterey, California 93940

ABSTRACT

A three dimensional staggered grid model, based on the Boussinesq equations, is developed and applied to mesoscale waves. The model is tested with a three-dimensional stable gravity wave and forecasts for 40 time steps are compared with the analytic solutions and also with a full grid model. Comparisons show very good agreement with both forecasts for the stated time. Failure of the relaxation scheme to meet the convergence criterion after 47 time steps is discussed.

DD FORM 1 NOV 65 1473 (PAGE 1)

S/N 0101-807-6811

Security Classification

A-31408

KEY WORDS	LINK A		LINK B		LINK C	
	ROLE	WT	ROLE	WT	ROLE	WT
oussinesq Equations						
taggered Grid Model						
esoscale Convection						
hree Dimensional Primitive Equations						

Thesis
B7958 Bozich
c.1
133636
A three dimensional staggered grid primitive equation model for application to mesoscale atmospheric motions.